Experiments on the 2 ^3P state of helium. IV. Measurement of the 2 $^3P_0$-2 $^3P_2$ fine-structure interval

W. Frieze, E. A. Hinds, and V. W. Hughes
Gibbs Laboratory, Physics Department, Yale University, New Haven, Connecticut 06520

F. M. J. Pichanick
Department of Physics and Astronomy, University of Massachusetts, Amherst, Massachusetts 01003
(Received 4 August 1980)

The 2 $^3P_0$-2 $^3P_2$ fine-structure interval ν_{02} has been measured using the optical-microwave atomic beam magnetic resonance technique with the result $\nu_{02} = 31\,908.040$ (20) MHz (0.6 ppm). This is in excellent agreement with the sum of previous separate measurements of the 2 $^3P_0$-2 $^3P_1$ and 2 $^3P_1$-2 $^3P_2$ intervals, which gives $\nu_{02} = 31\,908.060$ (36) MHz, and establishes internal consistency for all the measurements. The most accurate comparison with theory is for ν_{01}, and we obtain the most accurate experimental value for this by subtracting the earlier measurement of ν_{12} from the present result for ν_{02}. The result is $\nu_{01} = 29\,616.844 \pm 0.021$ MHz (0.7 ppm) (experiment) compared to $\nu_{01} = 29\,616.914 \pm 0.043$ MHz (1.5 ppm) (theory). Alternatively our experiment can be regarded as an independent measurement of the fine-structure constant with the result $\alpha^{-1} = 137.036\,12$ (11) (0.8 ppm) which is consistent with the more accurate currently accepted value $\alpha^{-1} = 137.035\,963$ (15) (0.11 ppm).

I. INTRODUCTION

This paper reports a direct measurement of the 2 $^3P_0$-2 $^3P_2$ fine-structure interval in the helium atom. The result provides not only a more accurate value for the fine structure but is an important check of experimental consistency. Within combined experimental errors this result for the 2 $^3P_0$-2 $^3P_2$ interval should be the sum of the earlier measurements of the intervals 2 $^3P_1$-2 $^3P_2$, (reported in paper I[1] and adjusted in paper II[2]), and 2 $^3P_0$-2 $^3P_1$ (reported in the preceding paper III[3]). The present work was reported briefly in Ref. 4.

Our result was obtained by observing the microwave magnetic dipole transition 2 $^3P_0(m_J = 0)$-2 $^3P_2(m_J = 0)$ which is forbidden at zero magnetic field because $\Delta J = 2$. In the presence of a magnetic field the Zeeman Hamiltonian admixes states of different J and excitation of the transition is possible. The transition probability, which has an approximately quadratic field dependence, determines the amount of microwave power needed to perform the experiment. If the measurement were made at too high a field, however, the accuracy in determining the fine structure would be limited by our ability to measure the absolute value of the field and by our knowledge of the g values. We chose to measure the transition at a field of about 2 kG, at which the transition could be excited with an available source of microwave power, and yet the field could still be determined with adequate precision.

II. THEORY OF THE EXPERIMENT

The reader is referred to the preceding paper III, and references therein for details of the experimental method which employed the optical-microwave magnetic resonance technique with a beam of atoms in the metastable 2 ^3S state. The 2 ^3P state was excited in the C-field region of an atomic beam magnetic resonance apparatus. The relevant 2 ^3P Zeeman energy sublevels are illustrated in Fig. 1, and the arrow shows the observed transition.

It has been pointed out in the previous papers

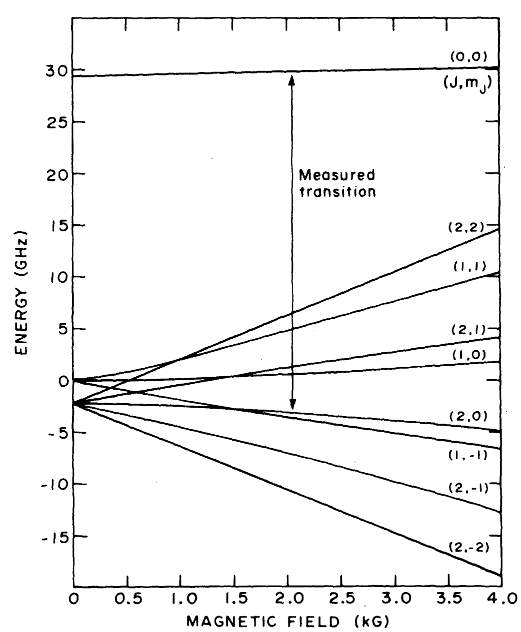

FIG. 1. Zeeman energy-level diagram of the 2^3P state of helium. The microwave transition observed in the present work is indicated, at the appropriate value of magnetic field, by a double arrow.

that our signal for a microwave transition between two $2\,^3P$ sublevels α and β is proportional to the product

$$[\sigma(m_S;\alpha)-\sigma(m_S;\beta)][\gamma(\beta;m_S')-\gamma(\alpha,m_S')],$$

where $\sigma(m_S;\alpha)$ is the relative excitation probability from the initial $m_S(=0)$ sublevel in the $2\,^3S$ beam to a $2\,^3P$ sublevel α, and $\gamma(\alpha,m_S')$ is the relative probability for decay to the final $2\,^3S$ sublevel $m_S'(=1)$ from a $2\,^3P$ sublevel α. It is crucial therefore that $\sigma(m_S;\alpha)$ be different from $\sigma(m_S;\beta)$ and that one of them be relatively large.

In this respect the present experiment on the $2\,^3P_0$-$2\,^3P_2$ interval is at an advantage relative to the experiment on the $2\,^3P_0$-$2\,^3P_1$ interval described in the preceding paper. That is because the $(J,m_J)=(2,0)$ state is strongly excited from $(m_S=0)$ in this experiment while the (1, 0) state used in the preceding experiment was suppressed by the $\Delta J=0$, $m_J=0$ not going to $m_J=0$ selection rule in zero magnetic field. In each case the (0, 0) state was excited by the small peak of the lamp spectrum which was smaller by a factor R ($R\simeq 0.4$) than the main peak. In fact one can show using the theory outlined in I that, under conditions of equal microwave-transition probability, our relative signal intensity was larger than that of the previous work by the approximate factor

$$(2-R)/R\sim 4\,.$$

The variation of signal with magnetic field is shown in Fig. 2 for $m_S=0$, $m_S'=+1$. In computing this curve we approximated experimental conditions by a choice of microwave-transition probability corresponding to the measured linewidth of 7.6 MHz and light intensity such as to give unit probability of optical excitation. In our calculations we took into account the spatial variation of the microwave magnetic field. We also treated the effects of multiple optical excitations which was not done in the previous papers. This had a small effect on the estimate of signal size. The time-independent part of the magnetic dipole matrix element for the microwave transition is $\mu_B H_1 V$ in the notation of I. $|V|$ is shown in Fig. 3 as a function of magnetic field. In the 2-kG field which we used, it had a value of about 0.35.

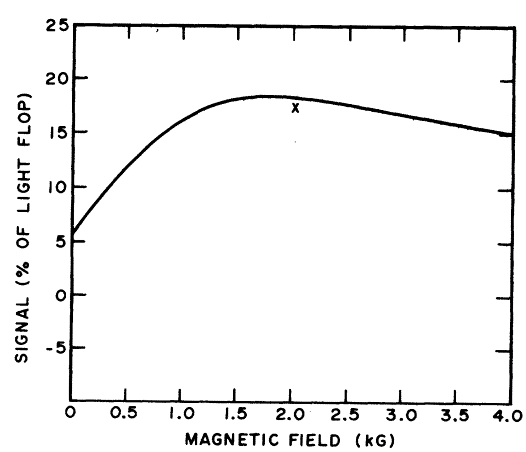

FIG. 2. Variation with magnetic field of the calculated microwave $2\,^3P$ signal for $2\,^3S$, m_S trajectory $0\to+1$. The signal is expressed as a percentage of the light flop, the number of atoms optically transferred from $m_S=0$ to $m_S=1$ in the absence of microwave power. The cross shows the observed signal.

III. APPARATUS

The apparatus used for this measurement was identical in many respects to that already described in II and III. Significant modifications were made to four systems: (A) the nuclear magnetic resonance (NMR) locking system for the magnetic field; (B) the subsidiary microwave system to measure the $2\,^3S$ Zeeman splitting as an absolute magnetic field calibration; (C) the microwave system for the $2\,^3P_2$-$2\,^3P_0$ resonant transition; (D) an on-line computer system to control data acquisition.

A. Nuclear magnetic resonance

The experiment required that the 2.036-kG magnetic field be stable and reproducible to better than 1 ppm. This was achieved by locking the magnet to a newly built proton NMR magnetometer. The NMR probe was of the traditional design

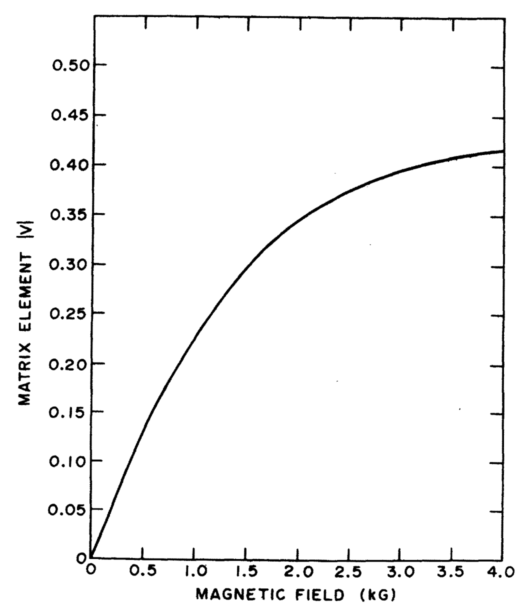

FIG. 3. Variation with magnetic field of the time-independent part of the matrix element coupling the $2\,^3P$ sublevels involved in the microwave transition.

with mutually orthogonal transmitter, receiver, and magnetic field modulation coils around a sample of mineral oil, and was located by the side of the main microwave cavity. The transmitter was driven by a frequency synthesizer operating at 8.671 MHz with-10-dBm output power. The receiver was connected through a high gain tuned preamplifier to a radio frequency lock-in amplifier, referenced to the transmitter signal. The output of this amplifier, which was proportional to the phase shift between transmitted and received signals, could have been used directly as our NMR signal. However, we chose to improve the signal-to-noise ratio further with the use of magnetic field modulation coils and a second lock-in amplifier operating at 60 Hz. After careful adjustment of the relative orientation of transmitter and receiver coils we were able to obtain a signal-to-noise ratio as high as 1000:1 at the peak of the NMR line in a 0.1 Hz bandwidth. A typical NMR line is given in Fig. 4. No detailed studies of the line shape were made, except to verify its reproducibility, since this line was used to stabilize the magnetic field but not to determine its absolute magnitude.

The magnet is designed for stabilization by a Hall probe and typically this arrangement is stable to 5 ppm at 2 kG. Our feedback connection, which allowed the NMR signal to regulate the magnet power supply, was a small coil wound on the Hall probe. The resulting system was stable to better than 0.05 ppm rms in eight hours and was reproducible within 0.02 ppm. The method of absolute calibration is discussed in the next section.

B. $2\,^3S$ state microwave system

Two shorted coaxial lines, shown in Fig. 5, were used to induce the $2\,^3S$ Zeeman transition

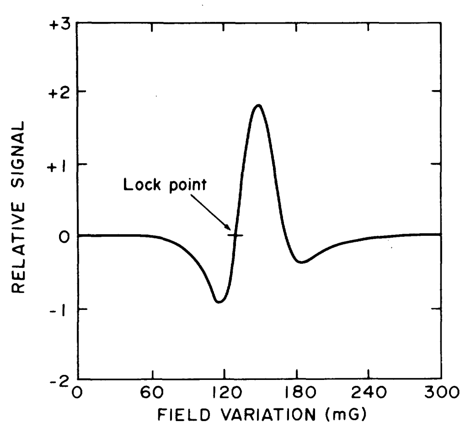

FIG. 4. Line shape of the NMR signal used to stabilize the magnetic field.

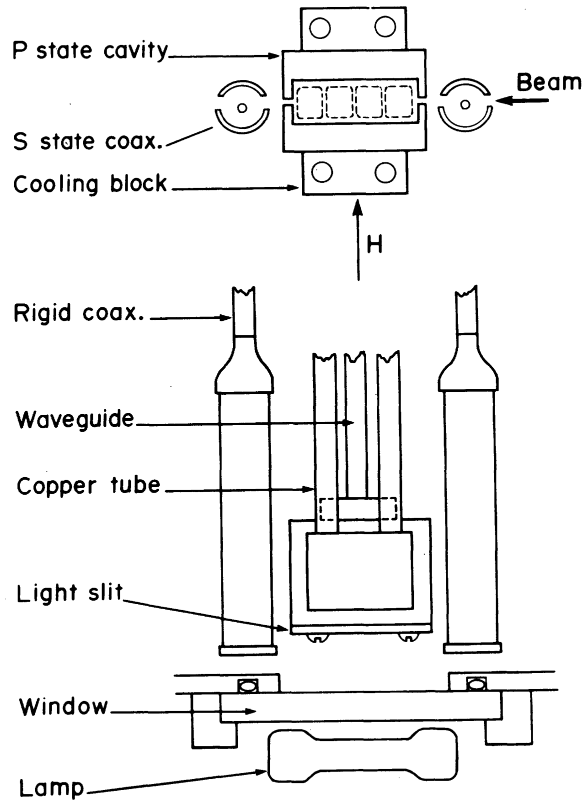

FIG. 5. Illustration of the microwave cavities used to excite the $2\,^3S$ and $2\,^3P$ transitions, and the discharge lamp used for the optical $2\,^3S-2\,^3P$ transition. The directions of the atomic beam and magnetic field are indicated. Microwave magnetic field lines in the $2\,^3P$ cavity are shown.

in the beam, the frequency of which provided a precise measurement of the magnetic field strength. These were made moveable so that maps of the field strength could be made along the beam axis. Since the NMR system was always used to lock the field, these measurements constituted a calibration of the NMR frequency.

The oscillator for the $2\,^3S$ resonance was a commercial reflex klystron, phase-locked at 5.707 GHz and amplified by a traveling wave tube. A schematic of the $2\,^3S$ state microwave system is given as Fig. 6.

C. $2\,^3P$ state microwave system

The $2\,^3P$ state resonance microwave cavity was a rectangular copper structure operating in the TE-410 mode at 32.99 GHz with a Q of 6500. Figure 5 illustrates the cavity and the microwave magnetic field. The cavity was clamped between water-cooled blocks to prevent thermal drifts of its resonant frequency. Power (25 W) was coupled in through a circular iris in the top. Pumping

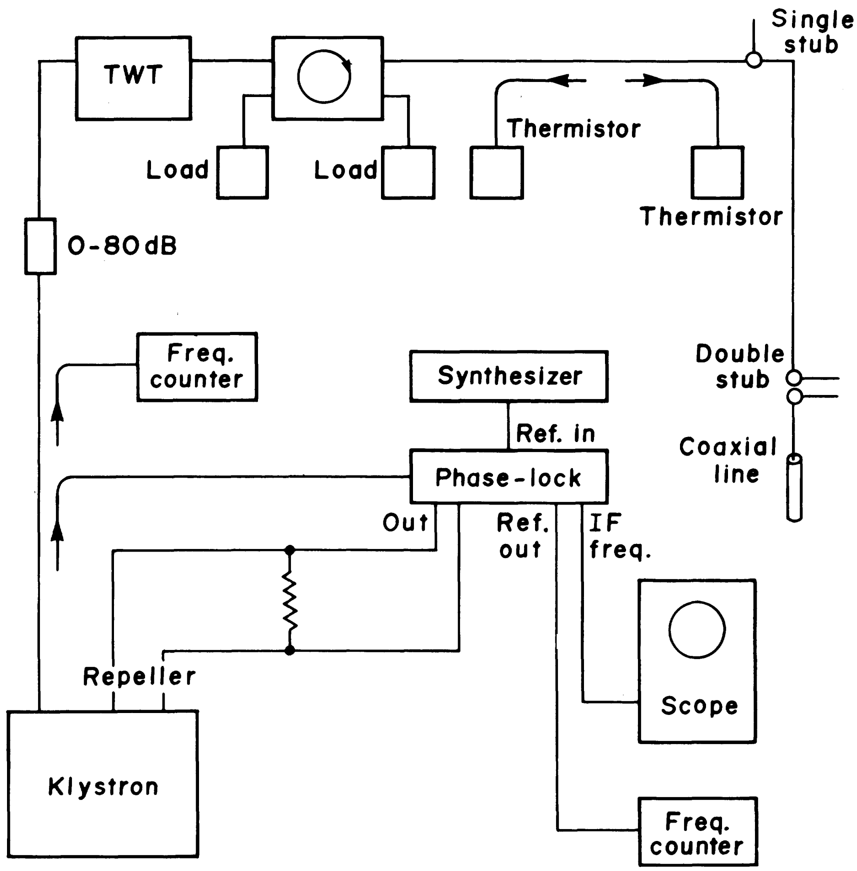

FIG. 6. Block diagram of the frequency stabilized, 6 GHz system used in the $2\,^3S$ transition.

light from the helium lamp entered through a narrow slot in the bottom of the cavity, parallel to the beam. The inside of the cavity was polished and silvered to improve its reflectivity.

Both $2\,^3S$ and $2\,^3P$ microwave structures were mounted on a common support plate which could be rotated and translated to allow alignment with the beam. In addition, the plate was translated along the beam when making field maps as described in Sec. III B.

The 32.99-GHz microwave radiation was generated by an extended interaction oscillator[5] capable of supplying up to 75 W over a ± 750-MHz range and voltage tuneable by ± 100 MHz. When free running, this tube was remarkably stable; the variations observed were roughly 3 ppm in frequency and 0.5% in power. During the experiment the tube was phase locked but power leveling was not needed.

A schematic of the $2\,^3P$ state microwave system is given in Fig. 7. In order to protect the tube from reverse power, we employed both a ferrite circulator and a thyratron crowbar triggered by a reverse power detector. The circulator had the additional feature that the power coupled to its unused fourth port was sufficient to operate a microwave frequency stabilizer which we used to phase lock the tube to a frequency synthesizer. The absolute microwave frequency was known to 0.05 ppm.

In order to modulate the microwave power for phase sensitive detection of the resonance signal, the anode voltage of the oscillator was switched through 500 V by means of a reed relay driven under computer control. This was a sufficient change to stop oscillation while altering the net current drawn by the tube by only about 10%. The relay was switched once every five seconds, with phase lock automatically re-establishing itself after 100–200 *ms*. To ensure that data were taken only after a stable lock had been achieved, counting was gated off for 500 *ms* after each relay transition.

D. On-line computer

The primary purpose of the computer was to generate square-wave modulation signals and to store data in synchronism with them. Figure 8

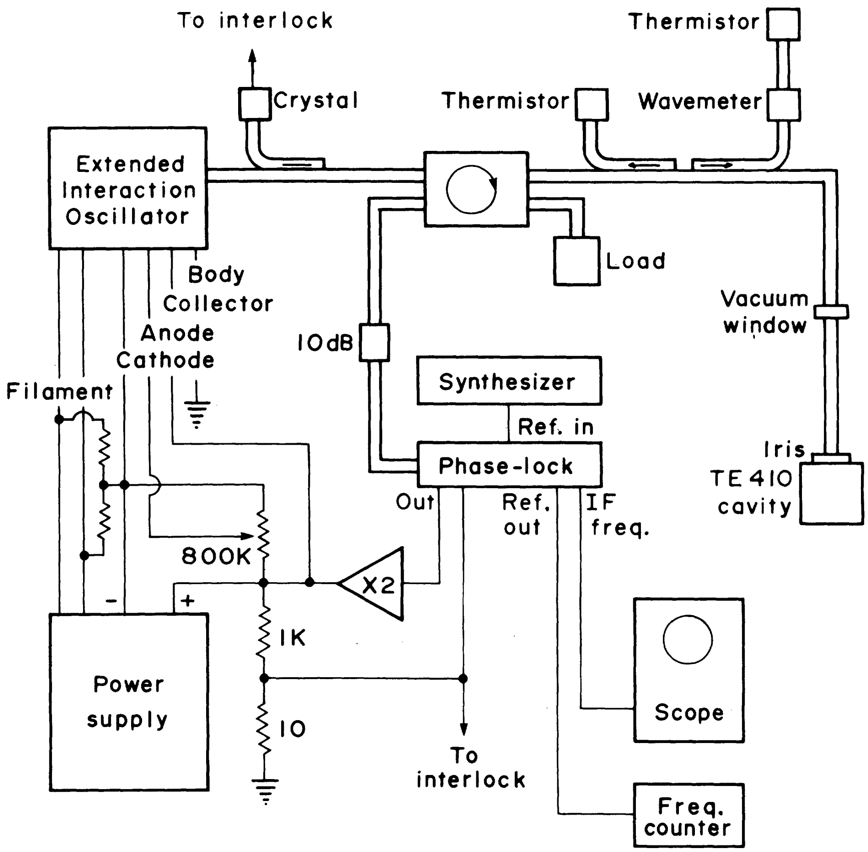

FIG. 7. Block diagram of the frequency stabilized, 30 GHz system used in the $2\,^3P$ transition.

shows the waveforms used to operate a shutter for the lamp and to modulate the microwave power. The modulations were effective in suppressing linear drifts in lamp intensity and microwave power. The $2\,^3P$ microwave resonance signal was recorded as a fraction of the light flop, and less time was needed to record the latter since it was relatively large. Counts were not recorded during the actual switching because of transient effects. The readout of each data point was the average of 30 sets of counts, and the computer generated a standard deviation of the mean which was checked against statistics. This demonstrated that the suppression of drifts and fluctuations was satisfactory.

IV. EXPERIMENTAL PROCEDURE

A. Beam studies

The composition of the beam was comparable to that described in III. Approximately one half of the beam was $2\,^3S$ atoms, the remainder consisting of $2\,^1S$ and photons. The total number of $2\,^3S$ ($m_J = 0$) atoms was recorded as 5×10^3 pulses per second (pps), the light flop was 160 pps and the $2\,^3P$ microwave signal was 28 pps.

B. Magnetic field measurement

The $2\,^3S$ Zeeman resonance was used to calibrate the NMR system and to provide a map of the magnetic field over the region of interest. An example of such a map is illustrated in Fig. 9. The error bars represent a conservative estimate of the systematic uncertainty in determining the $2\,^3S$ resonance line center which arose from a small asymmetry in the line shape. The nature of the field map did not change significantly during the entire period of data runs. In Fig. 9 the point denoted by *reference position* was the normal location of the $2\,^3S$ loop against which the NMR probe was calibrated during data runs. Since the $2\,^3P$ microwave cavity was normally located in the region between -0.50 in. and $+0.50$ in., a small correction was needed to compensate for the spatial variation between the reference position and the cavity position. It was found that the material of the microwave cavity had a small magnetic susceptibility for which an additional correction

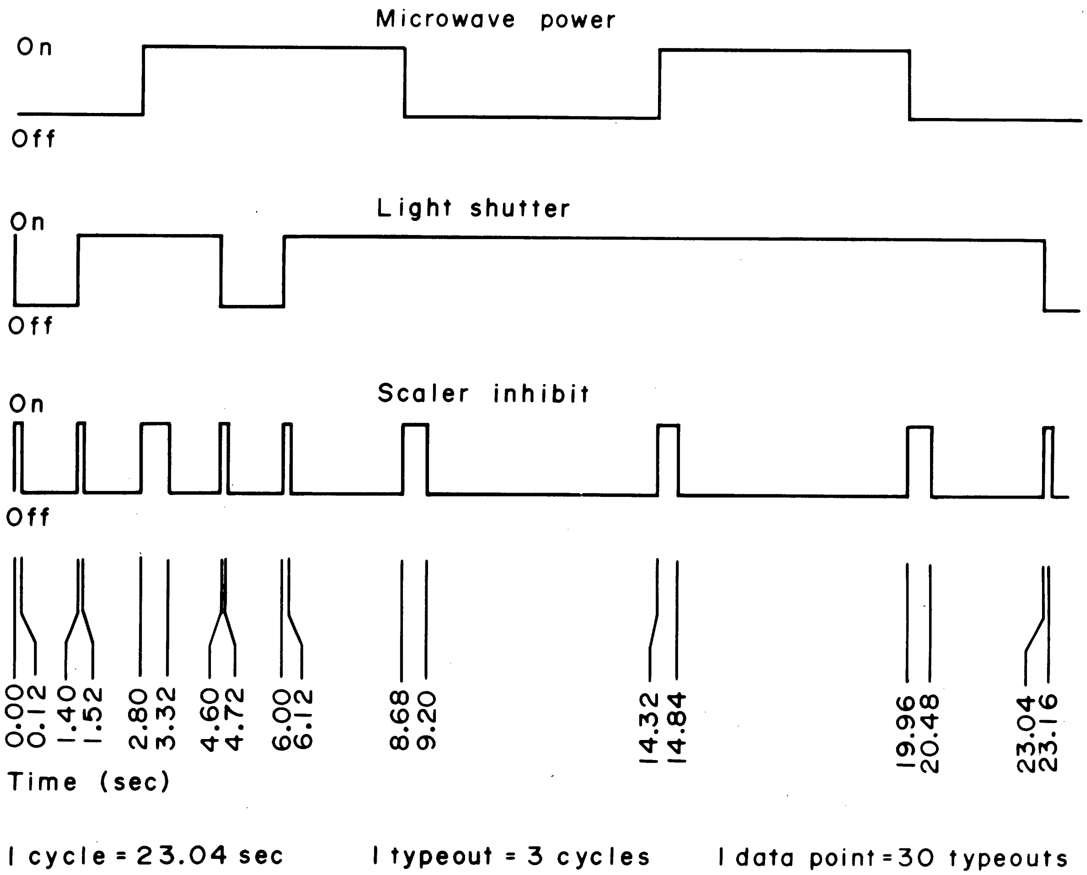

FIG. 8. Computer generated waveforms used to modulate the light flop and 2^3P transition signal. Scaler inhibit indicates the periods during which signals were not recorded because of switching transients.

was needed. This correction was obtained from direct measurements with and without the cavity using an NMR probe. The sign is that of a paramagnetic shielding correction which we assume

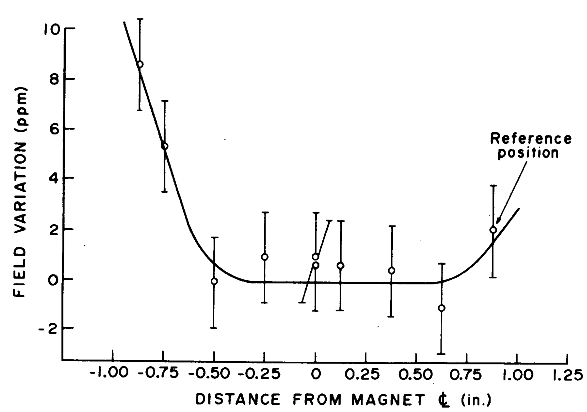

FIG. 9. Map of the magnetic field in the resonance region. During runs the 2^3S Zeeman measurements, used to calibrate the NMR system, were made at the point marked reference position.

arose from magnetic impurities in the copper walls of the cavity, pure copper being diamagnetic.

C. Resonance data collection

Our $2\,^3P$ state resonance data consisted of six runs, with fifteen data points per run. In addition, a $2\,^3S$ resonance curve was taken before and after each $2\,^3P$ state run. A typical run, which lasted about eight hours, produced an accuracy of about 1.5 ppm in the fine-structure determination, which represents 45 kHz in frequency units or about one per cent of the linewidth.

The majority of our data were clustered near the half maximum points to maximize their effectiveness in determining the line center. The data points were taken in a sequence which was symmetric with respect to the line center in order to minimize any problems due to drifts. When using a modulation system such as ours, one expects the background outside the resonance line to be zero. On several occasions, background was checked at fields far from the line center and we verified that it was in fact zero.

TABLE I. Summary of experimental runs and fitted results.

	Height (% of Light Flop)	Width (kHz NMR)	Center (kHz NMR)	ν_{02} (MHz)	χ^2/degree of freedom
Run #1	16.5 ± 1.9	39.4 ± 2.6	8672.13 ± 0.20	31 908.140 ± .042	0.76
Run #2	15.5 ± 1.8	32.9 ± 1.9	8672.45 ± 0.16	31 908.071 ± .034	0.73
Run #3	18.5 ± 1.9	36.2 ± 2.2	8672.11 ± 0.19	31 908.144 ± .040	1.23
Run #4	17.8 ± 2.0	34.9 ± 2.3	8672.57 ± 0.21	31 907.045 ± .046	0.96
Run #5	18.6 ± 1.9	36.2 ± 2.1	8672.40 ± 0.22	31 908.082 ± .046	0.73
Run #6	19.1 ± 2.1	38.6 ± 2.5	8672.32 ± 0.22	31 908.099 ± .047	1.13
Uncorrected Average	17.8 ± 0.8	36.4 ± 0.9	8672.33 ± 0.08	31 908.097 ± .017	

V. DATA ANALYSIS

A. Line fitting

The line-fitting procedure differed somewhat from that used in the previous paper. A Lorentzian line shape was used for the signal having the form

$$\rho(\alpha,\beta)=\frac{A(H)}{(\omega_{\alpha\beta}-\omega)^2+B(H)+\gamma^2}. \quad (1)$$

$A(H)$ and $B(H)$ are functions which depend on the magnetic field H. Their field-dependence can be predicted from theory, and the inclusion of this dependence in the line shape was our way of making the "slope correction" described in the previous paper. $\omega_{\alpha\beta}$ is the energy-level separation in the magnetic field H expressed in angular frequency units, ω is the angular frequency of the klystron, and γ is the radiative decay rate of the $2\,^3P$ state.

The first step in our fitting procedure was to assume a trial value ν_t for the fine-structure interval at zero magnetic field and to calculate from ν_t a magnetic field H_t at which the microwave frequency would equal the energy-level separation. This allowed us to make the following truncated Taylor expansion

$$\omega_{\alpha\beta}-\omega=a(\nu_{02}-\nu_t)+b(\nu_{02}-\nu_t)^2+c(H-H_t), \quad (2)$$

where ν_{02} is the fine-structure interval being measured. The expansion includes enough terms for our purpose and the values of the coefficients a, b, c were computed with sufficient accuracy from the theory of the Zeeman effect and previously measured values of the fine-structure intervals.

Three fitting parameters were used. They were the values of A and B at the magnetic field H_t and $(\nu_{02}-\nu_t)$, the correction to our trial value of the fine-structure interval. The data were fitted to the theoretical line shape Eq. 1 using the nonlinear least-squares method.

Table I summarizes the experimental runs and the fitted results. The values of χ^2 obtained from the fitting procedure are fully compatible with statistical fluctuations of the detected beam. Data from one run are shown in Fig. 10 together with the fitted theoretical line and the results of all the runs are compounded in Fig. 11. Table II lists two systematic adjustments which have to be made to the uncorrected average given in Table I. The first allows for the difference between the magnetic field at the $2\,^3S$ reference position (Fig. 9) and that in the microwave resonance region. The other correction takes into account the small magnetic susceptibility of the microwave cavity. Both corrections are discussed in more detail in Sec. IV B.

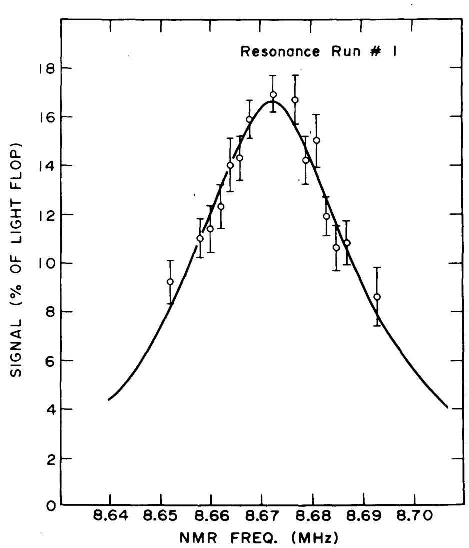

FIG. 10. Observed signal points and fitted line shape for a single run on the $2\,^3P$ transition as a function of magnetic field. The error bars represent 1σ, based on observed fluctuation of the signal.

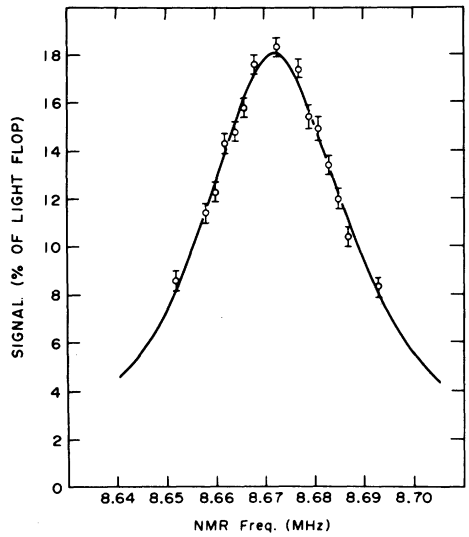

FIG. 11. Composite $2\,^3P$ transition line shape for all the experimental runs. Error bars represent 1σ, based on observed fluctuation of the signal.

B. Uncertainties

The experimental uncertainties are summarized in Table II. The largest contribution came from counting statistics, and this uncertainty could have been reduced by taking more data. Unfortunately, this was not possible because the microwave tube failed after six runs. The only other significant contribution to the uncertainties was in the expression $g_S' - g_L'$ involving the Zeeman g factors. Our knowledge of these could be improved by further experimentation.

VI. RESULTS AND CONCLUSIONS

The corrected result for the ν_{02} is compared below with the sum of the results for the intervals ν_{01}, (III, preceding paper) and ν_{12} (I and II):

Present measurement

31 908.040 (20) MHz,

Sum of earlier measurements

31 908.060 (36) MHz.

It can be seen that an excellent internal consistency has been established for the experiments and an overall improvement in precision has been achieved. The current state of the theory has been summarized in Table II of the preceding paper. The most accurate theoretical number is for the interval ν_{01}, so that the best comparison with theory is to subtract the previously measured interval ν_{12} from the present result for ν_{02}:

$$\nu_{01} = 29\,616.914\ (43)\ \text{MHz}\ (1.5\ \text{ppm})\quad \text{theory (Ref. 6)}$$

$$= 29\,616.844\ (21)\ \text{MHz}\ (0.7\ \text{ppm})\quad \text{experiment.}$$

The agreement is satisfactory, and any more detailed comparisons with theory would require the evaluation of terms of order α^5 Ry and $\alpha^3 m/M$ Ry. These measurements of the $2\,^3P$ fine-structure intervals in helium probably could be improved by at least a factor of 3 using the spectroscopic method of this paper. An alternative approach is to use the theory to obtain a value for the fine-structure constant from our result. This gives $\alpha^{-1} = 137.036\,12\ (11)\ (0.8\ \text{ppm})$ compared to the more accurate currently accepted value $\alpha^{-1} = 137.035\,963\ (15)\ (0.11\ \text{ppm})$.[7]

TABLE II. Systematic corrections and experimental uncertainties.

	MHz
Uncorrected fine structure ν_{02}	31 908.097
Magnetic field reference correction	−0.035
Magnetic shielding correction	−0.022
Corrected fine structure ν_{02}	31 908.040
Statistical uncertainty	0.017
Absolute field measurement uncertainty	0.003
Magnetic shielding correction uncertainty	0.003
Geometrical field average error uncertainty	0.002
Error on $(g_S' - g_L')$	0.007
Error on ν_{21} value	0.001
Quadrature sum of errors	0.020

VII. ACKNOWLEDGMENT

We are indebted to Robert Fong-Tom for his substantial contribution to the microwave engineering. This research was supported in part by the National Science Foundation under Grant No. PHY78-25655.

[1]F. M. J. Pichanick, R. D. Swift, C. E. Johnson, and V. W. Hughes, Phys. Rev. 169, 55 (1968), referred to as I.

[2]S. A. Lewis, F. M. J. Pichanick, and V. W. Hughes, Phys. Rev. A 2, 86 (1970), referred to as II.

[3]A. Kponou, V. W. Hughes, C. E. Johnson, S. A. Lewis, and F. M. J. Pichanick, Phys. Rev. A 24, 264 (1981), preceding paper, referred to as III.

[4]W. E. Frieze, E. A. Hinds, V. W. Hughes, and F. M. J. Pichanick, Phys. Lett. A78, 322 (1980).
[5]Varian Associates Model VKQ 2417.
[6]M. L. Lewis and P. H. Serafino, Phys. Rev. A 18, 867 (1978).
[7]E. R. Williams and P. T. Olsen, Phys. Rev. Lett. 42, 1575 (1979).